MSc in Photonics

PHOTONICS**BCN**

Universitat Politècnica de Catalunya (UPC)
Universitat Autònoma de Barcelona (UAB)
Universitat de Barcelona (UB)
Institut de Ciències Fotòniques (ICFO)

http://www.photonicsbcn.eu

Master in Photonics

MASTER THESIS WORK

Spatially variant polarized beams with tailored profiles

Maluenda Niubó, David

Supervised by Dr. Artur Carnicer, UB

Presented on date 5th September 2012

Registered at

Escola Tècnica Superior d'Enginyeria de Telecomunicació de Barcelona

Spatially variant polarized beams with tailored profiles

David Maluenda Niubó

Departament de Física Aplicada i Òptica, Universitat de Barcelona (UB), Martí i Franquès 1, Barcelona 08028 (Spain)

E-mail: dmalueni7@alumnes.ub.edu

Abstract. A new approach for the generation of spatially-variant polarized beams has been developed by manipulating vertical and horizontal field component of the optical signal individually in a Mach-Zehnder interferometric setup employing two liquid crystal spatial light modulators. After some simulations, the optical system has been mounted and the modulators have been calibrated. By using double pixel holograms two semi-full complex modulations has been achieved and their combination has let to obtain several spatially-variant polarization beams.

Keywords: spatial light modulator; computer generated holograms; spatially variant polarization; double pixel hologram.

1. Introduction

For many years polarization has become a very significant property of light. Its propagation and its interaction with matter has been extensively explored and analyzed in many ways [1]. While past studies mainly dealt with spatially homogeneous polarization states such as linear, circular and elliptical polarization, in recent years interest in spatially variant polarized beams (SVPB) has increased significantly due to their special abilities and properties compared with homogeneously polarized beams. These peculiar properties are useful to expand the capability and enhance the functionality of optical systems.

With radial polarization, for instance, a laser beam can be focused to generate a strong longitudinal and non-propagating electrical field at the focal plane; in this case one can achieve a narrower spot than we obtain with a common homogeneous polarized beam [2, 3, 4, 5, 6]. Therefore, PSF can be controlled and hence, improvements in microscope resolution[7] or increased density for optical storage. Furthermore, it is possible to generate three dimensional polarization fields by ingenious polarization engineering[8], which is very useful for optical trapping and particle manipulation[9, 10].

The generation process of SVPBs is still a challenging task. While former techniques, which use birefringent plates, neutral filters and interferometric setups, do not allow two dimensional arbitrary polarization patterns [11, 12], liquid crystal spatial

light modulators (LCSLM) provide a spatial capabilities. They act as phase retarders and amplitude modulators [13], like common plates and filters but pixel by pixel. With that, we can use all the knowledge in the literature, such as Jones formalism, for each pixel.

Nowadays, one can find several approaches to obtain SVP beams [14, 15], however many of them are barely able to achieve certain polarization states. The aim of this work is to develop an optical system to generate SVPB in a more flexible way than other methods. This can be carried out encoding any elliptical polarization states in every pixel. The flexibility of the assembly is provided by the individual processing of the x- (horizontal) and y-component (vertical) of the incident beam and subsequent recombining in a Mach-Zehnder interferometric setup. Two LCSLMs are employed displaying double pixel computer generated holograms to manipulate the two components [16, 17, 18].

This paper is organized as follows. In section 2 we review the basic concepts regarding SVPB. In section 3 the optical setup for generating such beams is described. Section 4 presents the SLM characterization procedure. In section 5 the algorithm for calculating arbitrary complex-valued holograms is introduced, and a simulation of its functionality is showed in section 6. Finaly, some experimental results are presented in section 7 and to conclude, in section 8, the main conclusions are summarized.

2. Spatially variant polarized beams

The aim of this communication is to develop an optical setup for the generation of spatially variant polarization beams using two twist nematic liquid crystal spatial light modulators for displaying the holograms, as in [19, 20]. The presented method processes individually the x- and y-component of an incident laser beam to encode the complex transmissions

$$\begin{aligned} C_x(x,y) &= C_{x0}(x,y)\exp\left[i\phi_x(x,y)\right] \\ C_y(x,y) &= C_{y0}(x,y)\exp\left[i\phi_y(x,y)\right] \end{aligned} \tag{1}$$

$C_{x0}(x,y)$, $C_{y0}(x,y)$ and $\phi_i(x,y)$, $\phi_i(x,y)$ are the amplitude modulation and the phase shift in every point (x,y), respectively, with C_x for the x-component and C_y for the y-component. Therefore, the oscilation plane orientation in every point (x,y) is given by $\delta_{amp} = \tan^{-1}\left[C_{y0}(x,y)/C_{x0}(x,y)\right]$.

The design of a SVPB is descrived by the angular distribution of the oscilating plane orientation and the phase shift

$$\begin{aligned} \delta_{amp} &= k\theta + \theta_{amp} \\ \delta_{ph} &= l\theta + \theta_{ph} \end{aligned} \tag{2}$$

where θ is the azimuth of the polar coordinates and k, l and θ_{amp}, θ_{ph} are the topological charges and the initial angle and phase, respectively. Figure 1 shows three representative designs of SVPBs. The first one is a radial polarized beam, the second is the called star mode and the third is a cylindrical Laguerre-Gauss transverse mode $\mathrm{TEM}_{p=1,l=0}$ profile,

which has a inner gaussian spot with radial polarization surrounded by a ring polarized azimuthally.

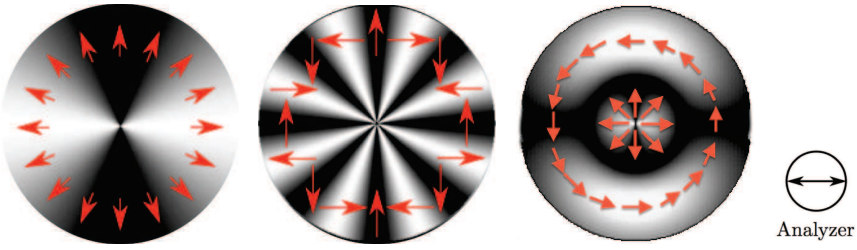

Figure 1. SVPBs design. (a) Radial mode ($k = 1$, $l = 0$, $\theta_{amp} = 0$ and $\theta_{ph} = 0$). (b) Star mode ($k = 0$, $l = 2$, $\theta_{amp} = \pi/2$ and $\theta_{ph} = 0$). (c) Core: Radial mode; Ring: Azimuthal mode ($k = 1$, $l = 0$, $\theta_{amp} = \pi/2$ and $\theta_{ph} = 0$).

3. Setup description

Figure 2 represents the experimental scheme of the approach developed for encoding spatially variant polarization states. The optical device is constructed in a Mach-Zehnder interferometric setup. A collimating lens aligns an expanded and unpolarized beam from He-Ne laser to propagate parallel along the optical path.

Since we are using an unpolarized laser, initial light has a undefined polarization state, for that reason the linear polarizer P_1 set at 45^o is required to define a well known polarization state

$$E_{in} = E_0 \exp\left[i\left(kz - \omega t + \phi_0\right)\right](\mathbf{i} + \mathbf{j}) \tag{3}$$

where E_0 is a constant, $k = 2\pi/\lambda$ and $\omega = 2\pi f$ are the wave number and the angular frequency, z and t are the propagation and temporal variables, respectively. ϕ_0 is the initial phase which is assumed $\phi_0 = 0$, $\mathbf{i}$ and $\mathbf{j}$ are the horizontal and vertical unitary vectors as well as i is the imaginary unit.

Then the beam is splited by PBS_1. Since the incident polarization direction is 45^o, the splited beams E_x and E_y have the same intensity. The oscillating plane of E_x is horizontal and vertical for E_y.

Reflected by the mirrors M_1 and M_2, both beams pass through half wave plates HWP, which rotate the oscillating plane to achieve the expected response of SLM. Afterwards, light passes through the liquid crystal spatial light modulators SLM_1 and SLM_2. Both modulators are Holoeye HEO 0017, which are twisted nematic liquid crystal displays, with a resolution of 1024×768 pixels and $32\,\mu m$ of pixel pitch.

PBS_2 has two functions. On the one hand it projects, as a linear polarizer, the outgoing light from SLMs. This is required because twist nematic LCSLM change the polarization of light. On the other hand, PBS_2 acts as a set of othogonal linear

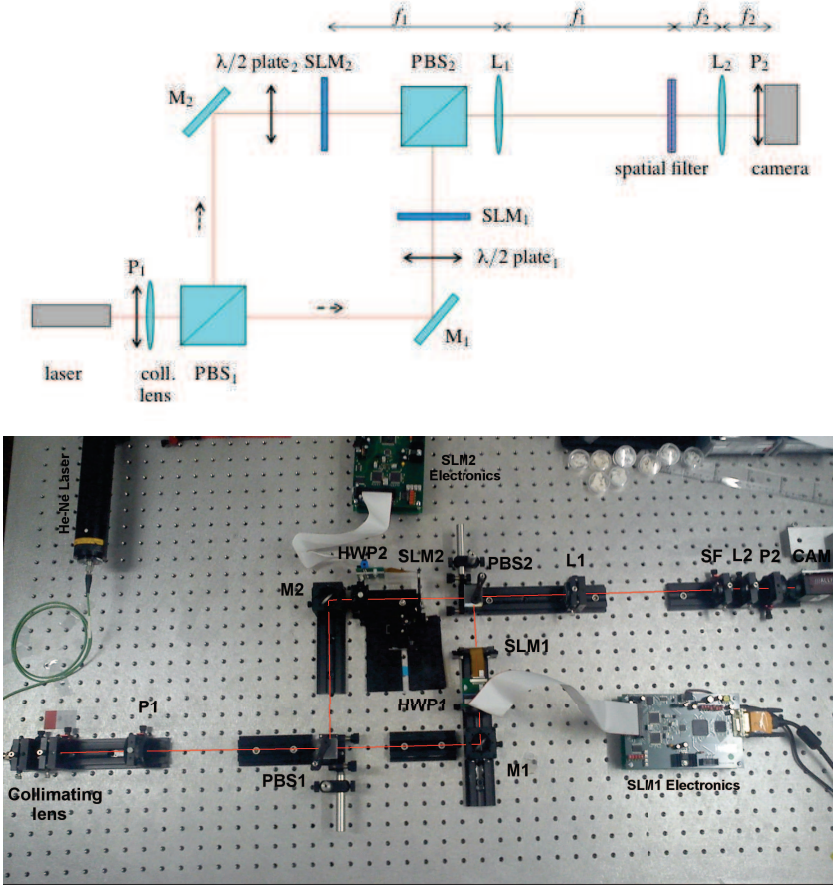

Figure 2. Schem and experimental setup to generate spatially variant polarized beams, based on a Mach-Zehnder interferometer.

polarizers to encode the x- and y-component independently by each interferometric arm after recombination. Consequently, the transmitted output signal can be written as

$$E_{out} = E_x h_x(x,y)\,\mathbf{i} + E_y h_y(x,y)\,\mathbf{j} \tag{4}$$

$h_x(x,y)$ and $h_y(x,y)$ are the specific tailored computer-generated phase holograms derivated in section 5 for x- and y-component, respectively.

The complex modulation introduced by the SLMs leads to a transmission signal that is reconstructed by the following Fourier lens system encodes the desired complex transmission. The reconstruction system consists of a $4f$ Fourier lens system. In the back focal plane of L_1 and at the same time the front focal plane of L_2 a circular pupil filter SF is placed. Its radius is responsible for the signal isolation and noise reduction while the reconstruction process. The encoded spatially-variant polarization beam can either be evaluated by the analyzer P_2 and the CCD camera or used for further applications.

4. Spatial Light Modulator characterization

SLMs have been characterized by using a procedure based on [21]. This procedure uses a cosinusoidal fringe pattern after a Mach-Zehnder interferometer to determine the phase shift introduced by each grey level.

Two parts are separated on the beam section by the SLM, the lower part (d) corresponds to the reference grey level ($gl = 0$) and the upper one (u) corresponds to the grey level to be characterized.

Since the fringes are aligned in the y or vertical direction, it is possible to represent their horizontal profiles by

$$\begin{aligned} I_u(x) &= a_u + b_u \cos[2\pi x/P + \phi_u] \\ I_d(x) &= a_d + b_d \cos[2\pi x/P + \phi_d] \end{aligned} \tag{5}$$

where $x = 0 \ldots N-1$, N is the number of pixels ($N = 400$). P is the period of the fringes (hich is related to their frequency by $f = N/P$), a_i ($i = d, u$) represents the background value and b_i is related to the contrast of the patterns.

Equations (5) work for every row in each zone and should be approximately equal for all of them, so we have analized only one for zone (marked in green on Figures 3(a) and 3(c)). In order to avoid the noise by non-uniformities, we have filtered the Fourier transorm of the profiles allowing to pass only the first two peaks corresponding to the frequency f. On Figure 3(b) and 3(d) is shown the reconstructed profiles after the filtering process. While on Figure 3(b) both cosinusoidals profiles are in-phase, on Figure 3(d) they are clearly out of phase. Consequently, it is easier to calculate the

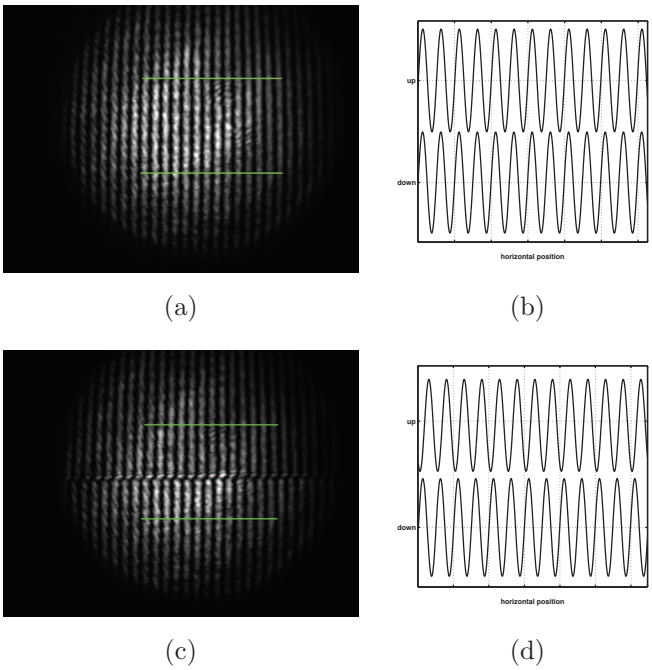

(a) (b)

(c) (d)

Figure 3. Mach-Zehnder interferences to obtain the phase shift introduced by SLM. (a) $gl = 0$ and (b) $gl = 100$ on the upper part and both with 0 grey level on the down, as reference.

relative fringe displacement Δ and the fringe period to compute $\phi = 2\pi\Delta/P$. For exemple, for grey level 100 the phase shift is $\phi_{100} = 0.79\,\pi = 142\,^o$, in comparation with grey level 0. On Figure 4(b) we can see the phase shift introduced by each grey level applied on the SLM.

In order to have identical experimental conditions, the amplitude modulation of the device are measured by profiting the same setup from the phase evaluation. The procedure is equal than explained before but blocking the arm of the interferometer where is not the SLM, therefore the fringe pattern disappears and the transmitance is given by

$$T = \mathcal{I}_u/\mathcal{I}_d \tag{6}$$

$\mathcal{I}_i$ is the mean of the grey values captured by the camera on each zone ($i = d, u$). We have used two parts on the beam section to avoid the error introduced by the intensity fluctuations of the laser.

Because the amplitude modulation is more useful information than tansmittance, on Figure 4(a) is shown the root square of the tranmittance. To sum up phase and amplitude modulation, on Figure 4(c) is depicted the polar curve where each point in the polar graph represent a grey level on the SLM, the radial distance corresponds to the amplitude modulation and the angle corresponds to the phase modulation.

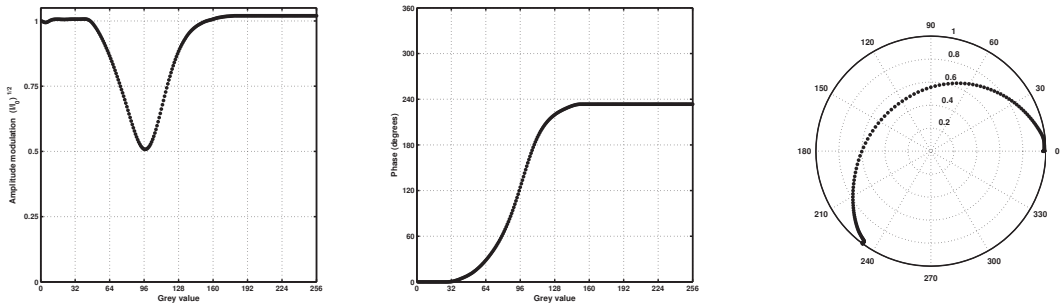

(a) (b) (c)

Figure 4. SLM response. (a) the amplitude modulation is presented as well as the phase modulation on (b). The polar graph (c) represent every grey level appliable by SLM and its response, in amplutude (radial distance) and in phase (angle).

5. Codification procedure

As is shown in the previous section, the SLMs is able to display different complex transmittances depending on the grey level sended to them, although this complex transmitance does not fill the entire complex plane at all. To generate a greater amplitude and phase modulation we have used the Arrizon codification procedure[16, 17, 18]. This method is based on cells (or macropixels) of two single pixels on a pixelated SLM.

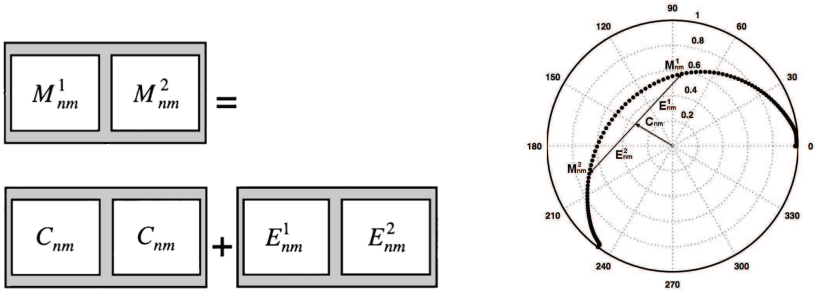

Figure 5. Double-pixel cel with signal and error components.

Double pixel hologram (DPH) procedure makes possible achieve an arbitrary complex modulation C by using the constrained complex modulation $M = C_0 \exp(i\phi)$ by SLM, following the relation

$$C_{nm} = \left(M^1_{nm} + M^2_{nm}\right)/2 \quad ; \quad E^1_{nm} = -E^2_{nm} \tag{7}$$

The complex values of M^1_{nm} and M^2_{nm} are obtained by the procedure illustrated on Figure 5. On the polar plot the secant crossing the complex point C_{nm} intersects the modulation curve at the complex points M^1_{nm} and M^2_{nm}. To fulfill Equation (7), the obliquity of this secant is chosen in such a way that C_{nm} coincides with the middle point between M^1_{nm} and M^2_{nm}.

Many values of the complex plane can be obtained in two points belonging to the modulation curve as shown in Figure 5. However, not all values in the complex plane can be achieved in this way. Figure 6 shows all values accessible, in particular, a subset of these values is within a semicircle of radius 0.5. Note that the diameter of the semicircle forms an angle of 30 ° relative to the arbitrary phase origin. Note that the available values form a discrete set. Since the transmittances $C_x(x, y)$ and $C_y(x, y)$ are continuous, is assigned the closest accessible value.

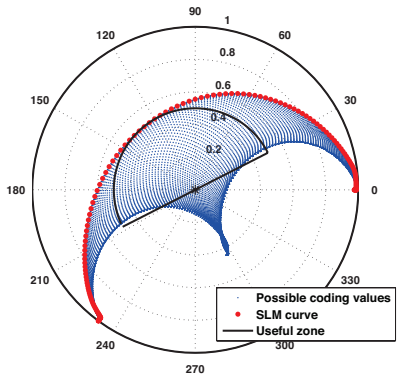

Figure 6. In red is represented the complex transmittance applicable by SLM. Complex transmittance after the combination of each couple of values belonging to SLM are in blue. The useful semi-full complex zone is enclosed by the black line.

6. Simulations

In order to see the functionality of the coding procedure, we have develop simulated the three examples of spatial-variant polarirated beams presented in section 2. First the beam is designed, it means how amplitudes and phases are arranged for each component. Secondly, this designed beam has to be implemented with the coding procedure described above. Third, holograms is Fourier transformed and the high frequencies are filtered, in order to simulate the $4f$ setup. Finally, the beam are reconstructed by means a second transforming.

The first two columns of Figure 7 present the holograms to generate the radial mode, the star mode and the cylindrical Laguerre-Gauss transverse mode $\mathrm{TEM}_{p=1,l=0}$ whit the radial mode inner and the azimuthal mode outer. The third and fourth colums are the $x-$ and y-component reconstruction.

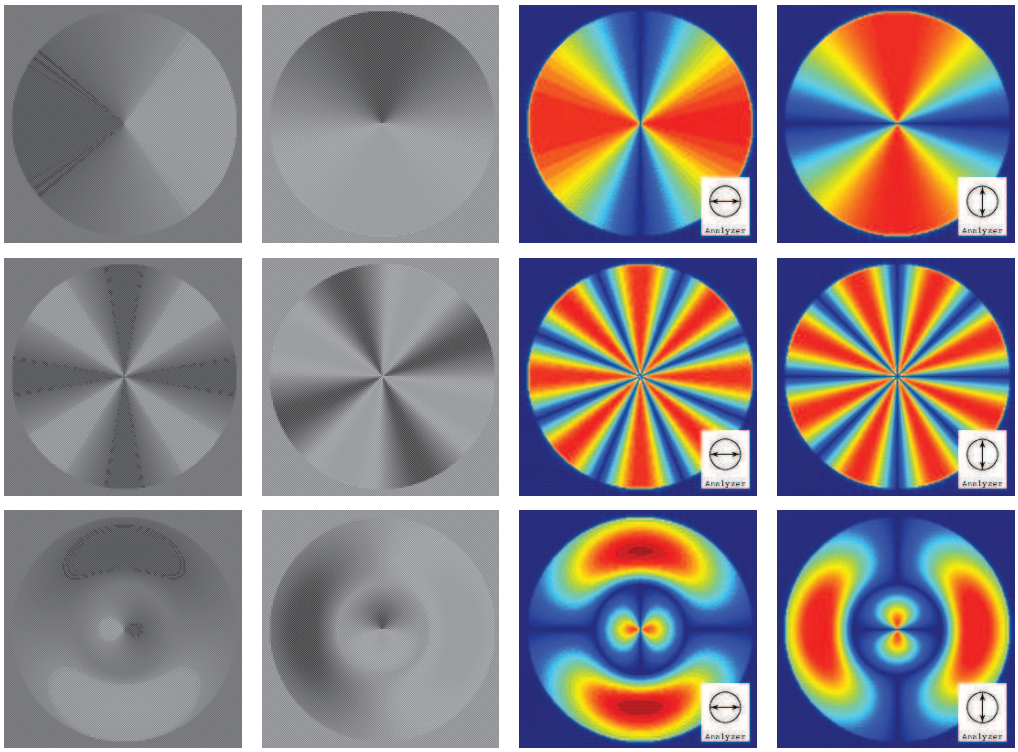

Figure 7. In the first and secon columns are represented the double pixel holograms for x- and y- components. In the third and fourth columns are presented the reconstruction after filtering high frequencies of their Fast Fourier Transform, respectively. First row refers to radial polarization. A *star* mode is in the second row. Finally and in the third is presented a TEM_{10}, where its core is radially and the crown is azimuthally polaraized.

7. Experimental results

Finally, we have implemented the spatial-variant polarized beams simulated in the previous chapter experimentally. The holograms shown on the Figure 7 have been applied on the two SLMs in the setup descrived in the third section. To analize the polarization of these beams, we have used a polarizer before the camera as is showed on Figure 8.

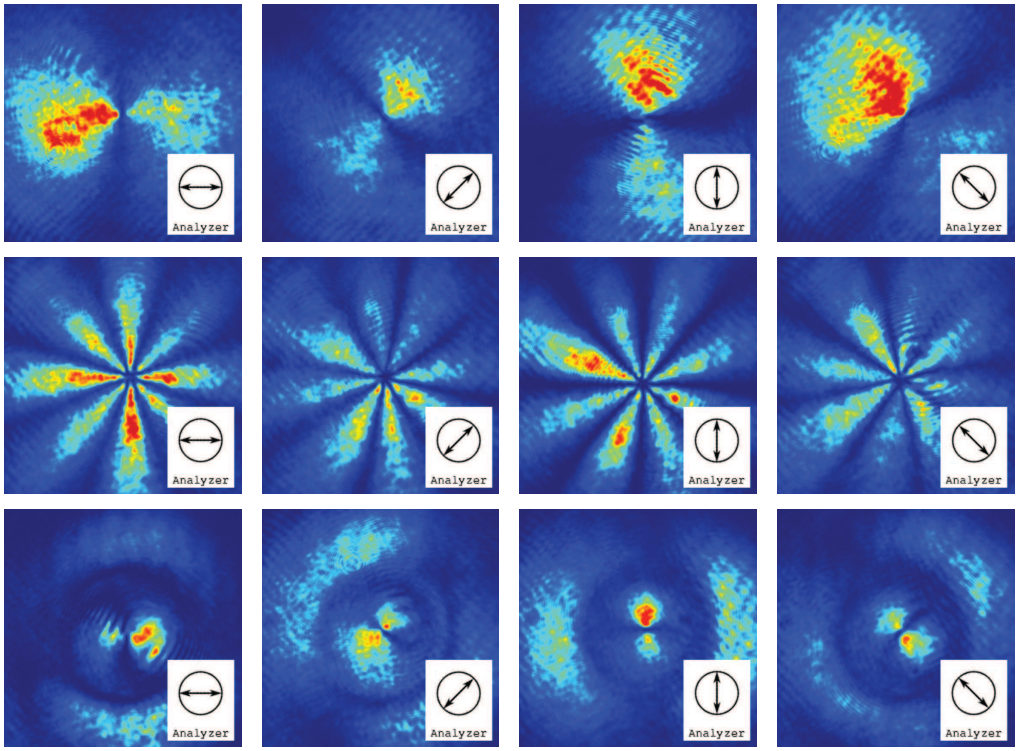

Figure 8. Experimental results of spatially variant polarized beams. In first row is presented the radial mode, the star mode is represented in the second row as well as the TEM_{10} mode in the third. Every column shows the beams analized at 0°, 45°, 90° and 135°, respectively.

8. Concluding remarks

An optical setup for generation spatially variant polarization beams using a Mach-Zehnder interferometer has been develop to modulate phase and amplitude on x- and y-component separately to implement any polarization state on every point on the section beam.

Even though the used SLMs have a phase modulation up to 1.3π with certain amplitude coupling, we have demostrated that full complex modulation is possible using two SLMs. To achieve this the double pixel hologram algorith has to be used.

On the one hand, the use of a Mach-Zenhder always involves many optical elements as well as their correct alligment becomes a fundamental issue. Every of this elements

introduces a wavefront distortion, that may be analized by a Shack Hartmann wavefront sensor and largely corrected by the SLMs. On the other hand, once the system is alligned some fluctuations appear for mechanical reasons like vibrations, small airflows or thermal dilatations due to the finesse of the system. Several of these issues have been avoided keeping the system insulated on a optical table for vibrations as well as in a box for a airflows.

To sum up, the results showed in the previous chapter prove that we are on the right way, although many improvements are required to generate a enhanced spatial variant polarized beams.

Acknowledgments

I am indebted to my advisor, Prof. A. Carnicer for his help and encouragement throughout the course of this work, as well as Prof. I. Juvells and Prof. S. Vallmitjana for their advices and support.

References

[1] Zhan Q 2009 *Advances in Optics and Photonics* **1**(1) 1–57
[2] Youngworth K and Brown T 2000 *Opt. Express* **7**(2) 77–87
[3] Dorn R, Quabis S and Leuchs G 2003 *Phys. Rev. Lett.* **91**(23) 233901
[4] Pereira S and Van de Nes A 2004 *Optics communications* **234**(1) 119–124
[5] Sheppard C and Choudhury A 2004 *Applied optics* **43**(22) 4322–27
[6] Lerman G and Levy U 2008 *Opt. Express* **16**(7) 4567–81
[7] Beversluis M, Novotny L, and Stranick S, 2006 *Opt. Express* **14**(7) 2650–56
[8] Abouraddy A and Toussaint Jr K 2006 *Phys. Rev. Lett.* **96**(15) 153901
[9] Zhan Q 2004 *Opt. Express* **12**(15) 3377–82
[10] Kawauchi H, Yonezawa K, Kozawa Y and Sato S 2007 *Optics letters* **32**(13) 1839–41
[11] Neil M, Massoumian F, Juskaitis R and Wilson T 2002 *Optics letters* **27**(21) 1929–31
[12] Tidwell S, Kim G and Kimura W 1993 *Applied optics* **32**(27) 5222–29
[13] Davis J, McNamara D, Cottrell D and Sonehara T 2000 *Applied Optics* **39**(10) 1549–54
[14] Eriksen R, Mogensen P and Glückstad J 2001 *Optics communications* **187**(4-6) 325–336
[15] Wang X, Ding J, Ni W, Guo C and Wang H 2007 *Optics letters* **32**(24) 3549–51
[16] Arrizón V 2003 *Optics letters* **28**(24) 2521–23
[17] Arrizón V, González L, Ponce R and Serrano-Heredia A 2005 *Applied optics* **44**(9) 1625–34
[18] Arrizón V 2003 *Optics letters* **28**(15) 1359-61
[19] Schaschek F 2011 *Treballs acadèmics UPC* `http://upcommons.upc.edu/pfc/handle/2099.1/12983`
[20] Carnicer A, Juvells I, Maluenda D, Martinez-Herrero R, M. Mejías P, Schaschek F 2012 *Proc. of SPIE* **8429** 84290Y
[21] Martín-Badosa E, Carnicer A, Juvells I and Vallmitjana S 1997 *Meas. Sci. Technol.* **8** 764–772